

# Altered Brain Glymphatic Flow at Diffusion-Tensor MRI in Rapid Eye Movement Sleep Behavior Disorder



Yun Jung Bae, MD, PhD • Jong-Min Kim, MD, PhD • Byung Se Choi, MD, PhD • Nayoung Ryoo, MD •  
Yoo Sung Song, MD, PhD • Yoonho Nam, PhD • In-Young Yoon, MD, PhD • Se Jin Cho, MD •  
Jae Hyoung Kim, MD, PhD

From the Departments of Radiology (Y.J.B., B.S.C., S.J.C., J.H.K.), Neurology (J.M.K.), Nuclear Medicine (Y.S.S.), and Psychiatry (I.Y.Y.), Seoul National University Bundang Hospital, Seoul National University College of Medicine, 173-82 Gumi-ro, Bundang-gu, Seongnam 463-707, Republic of Korea; Department of Neurology, Eunpyeong St Mary's Hospital, College of Medicine, The Catholic University of Korea, Seoul, Republic of Korea (N.R.); and Division of Biomedical Engineering, Hankuk University of Foreign Studies, Yongin, Republic of Korea (Y.N.). Received July 20, 2022; revision requested September 6; final revision received February 23, 2023; accepted March 13. **Address correspondence to** J.M.K. (email: [jongmin1@snu.ac.kr](mailto:jongmin1@snu.ac.kr)).

Y.J.B. is supported by a National Research Foundation of Korea grant funded by the Korean government (Ministry of Science and ICT) (no. 2022R1F1A1064530) and the Seoul National University Bundang Hospital research fund (grant 02-2021-0015).

Conflicts of interest are listed at the end of this article.

See also the editorial by Filippi and Balestrino in this issue.

Radiology 2023; 307(5):e221848 • <https://doi.org/10.1148/radiol.221848> • Content codes:  

**Background:** Brain glymphatic dysfunction may contribute to the development of  $\alpha$ -synucleinopathies. Yet, noninvasive imaging and quantification remain lacking.

**Purpose:** To examine glymphatic function of the brain in isolated rapid eye movement sleep behavior disorder (RBD) and its relevance to phenoconversion with use of diffusion-tensor imaging (DTI) analysis along the perivascular space (ALPS).

**Materials and Methods:** This prospective study included consecutive participants diagnosed with RBD, age- and sex-matched control participants, and participants with Parkinson disease (PD) who were enrolled and examined between May 2017 and April 2020. All study participants underwent 3.0-T brain MRI including DTI, susceptibility-weighted and susceptibility map-weighted imaging, and/or dopamine transporter imaging using iodine 123-2 $\beta$ -carbomethoxy-3 $\beta$ -(4-iodophenyl)-*N*-(3-fluoropropyl)-nortropane SPECT at the time of participation. Phenoconversion status to  $\alpha$ -synucleinopathies was unknown at the time of MRI. Participants were regularly followed up and monitored for any signs of  $\alpha$ -synucleinopathies. The ALPS index reflecting glymphatic activity was calculated by a ratio of the diffusivities along the x-axis in the projection and association neural fibers to the diffusivities perpendicular to them and compared according to the groups with use of the Kruskal-Wallis and Mann-Whitney *U* tests. The phenoconversion risk in participants with RBD was evaluated according to the ALPS index with use of a Cox proportional hazards model.

**Results:** Twenty participants diagnosed with RBD (12 men; median age, 73 years [IQR, 66–76 years]), 20 control participants, and 20 participants with PD were included. The median ALPS index was lower in the group with RBD versus controls (1.53 vs 1.72; *P* = .001) but showed no evidence of a difference compared with the group with PD (1.49; *P* = .68). The conversion risk decreased with an increasing ALPS index (hazard ratio, 0.57 per 0.1 increase in the ALPS index [95% CI: 0.35, 0.93]; *P* = .03).

**Conclusion:** DTI-ALPS in RBD demonstrated a more severe reduction of glymphatic activity in individuals with phenoconversion to  $\alpha$ -synucleinopathies.

© RSNA, 2023

Supplemental material is available for this article.

The glymphatic system is a highly organized waste clearance pathway that eliminates soluble proteins from the brain (1,2). In the perivascular channels formed by astroglial cells, the cerebrospinal fluid inflows along the periaxonal space, moves into the brain parenchyma through a mechanism facilitated by aquaporin-4 channels in astrocytic end-feet, and exchanges with interstitial fluid efflux toward the perivascular space (1,2). Consequently, glymphatic impairment has been linked to neurodegenerative disorders characterized by pathologic protein aggregation, such as Alzheimer disease and Parkinson disease (PD) (1–4).

Isolated rapid eye movement sleep behavior disorder (RBD) is parasomnia characterized by loss of normal muscle atonia during rapid eye movement sleep and by dream-enacting behaviors without underlying neurodegenerative disease and is considered as an important prodromal disease

for future  $\alpha$ -synucleinopathy (5–7). More than 80% of patients with RBD are at a risk of developing PD, dementia with Lewy bodies, or multiple system atrophy, with a phenoconversion rate of up to 6.3%–8% per year (8,9). The integrity of the glymphatic system in patients with RBD has been evaluated in a few previous studies (10–12). However, an evaluation of the role of the glymphatic dysfunction contributing to the phenoconversion of RBD with use of MRI remains lacking in the literature.

Most initial studies of human glymphatic drainage have used dynamic contrast-enhanced MRI followed by intrathecal or intravenous gadolinium-based contrast agent injection (13–16). Intrathecal contrast agent injection can demonstrate delayed clearance of the agent as evidence of glymphatic dysfunction but is an invasive procedure and restricted in some countries (13). Gadolinium-based contrast agent administration into the cerebrospinal fluid or

## Abbreviations

ALPS = analysis along the perivascular space, DTI = diffusion-tensor imaging,  $^{123}\text{I}$ -FP-CIT = iodine 123-2 $\beta$ -carbomethoxy-3 $\beta$ -(4-iodophenyl)-*N*-(3-fluoropropyl)-nortropane, PD = Parkinson disease, RBD = rapid eye movement sleep behavior disorder, SMWI = susceptibility map-weighted imaging

## Summary

Altered brain glymphatic flow at diffusion-tensor MRI in individuals with isolated rapid eye movement sleep behavior disorder may help predict the risk of phenoconversion to  $\alpha$ -synucleinopathies.

## Key Results

- In a prospective study of 60 participants, the median index using diffusion-tensor imaging analysis along the perivascular space (ALPS) reflecting perivascular brain glymphatic flow was lower in the groups with rapid eye movement sleep behavior disorder and Parkinson disease versus controls (1.53 and 1.49 vs 1.72;  $P < .001$ ).
- The risk of conversion to  $\alpha$ -synucleinopathy diseases decreased with an increasing ALPS index (hazard ratio, 0.57 per 0.1 increase in ALPS index;  $P = .03$ ).

repeated intravenous contrast agent injection can lead to gadolinium deposition in the brain (17,18). Considering these risks, glymphatic assessment without contrast agent is preferred, particularly for patients with progressive neurodegenerative disease.

Herein, we aimed to investigate glymphatic function in individuals with RBD with use of diffusion-tensor imaging (DTI) analysis along the perivascular space (ALPS) (19–24). DTI-ALPS allows the assessment of the glymphatic activity without intravenous or intrathecal contrast agent injection. The glymphatic function assessed with DTI-ALPS has been

shown to be correlated with that assessed with the direct intrathecal tracer-based measurement in humans (13,25). We hypothesized that a disrupted neuroprotective glymphatic system might be associated with the pathophysiologic abnormalities at the RBD stage, because RBD represents preclinical  $\alpha$ -synucleinopathy (6,7,9) and shows a lower percentage of N3 sleep stage, where the glymphatic system normally operates (Appendix S1) (1,4,26). Thus, our purpose was to evaluate brain glymphatic function in individuals with RBD and its relevance to phenoconversion to  $\alpha$ -synucleinopathy with use of DTI-ALPS.

## Materials and Methods

This prospective study was approved by the institutional review board of Seoul National University Bundang Hospital (institutional review board no. B-1610–368–303). Written informed consent was obtained from all participants.

## Study Participants

Between May 2017 and April 2020, consecutive patients were prospectively enrolled and examined by a neurologist (J.M.K.) with 21 years of experience in movement disorders. During this period, patients with clinically and polysomnographically diagnosed RBD, 1:1 age- (based on age at imaging) and sex-matched control participants, and 1:1 age- and sex-matched patients diagnosed with de novo PD were included (Fig 1).

First, a clinical diagnosis of RBD was made based on the standard guidelines of the International Classification of Sleep Disorders, third edition (Appendix S1) (27). Patients who underwent 3.0-T brain MRI suitable for DTI-ALPS and/

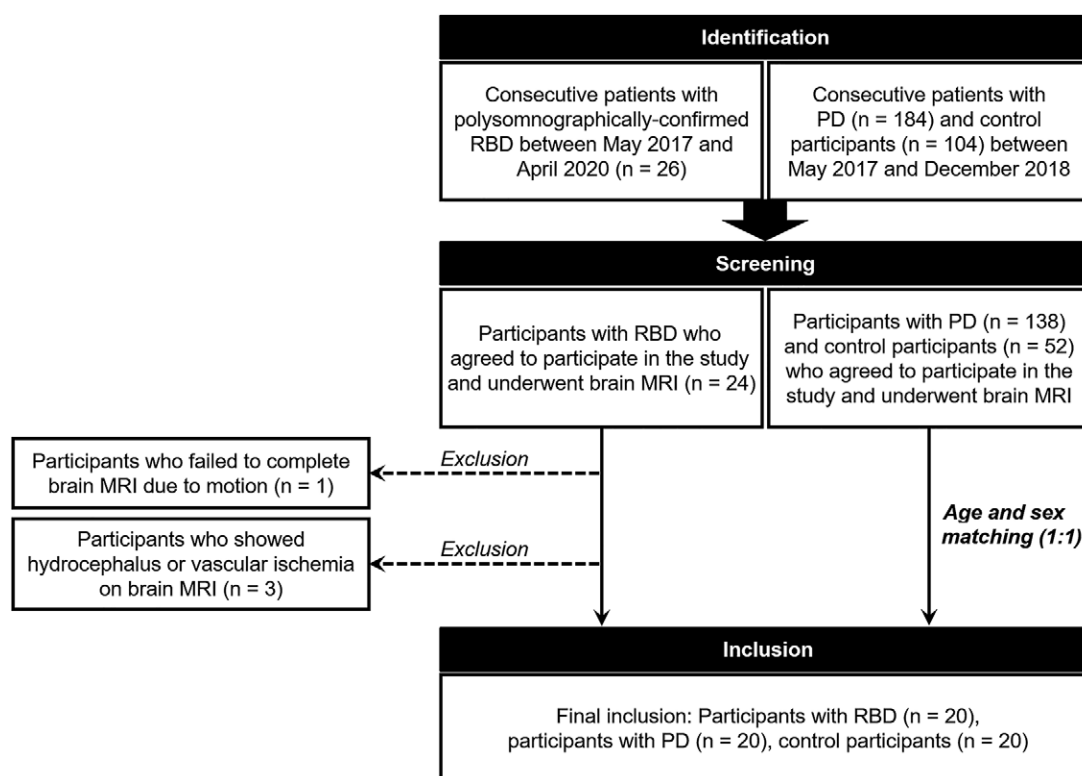


**Figure 1:** Flow diagram of the study sample. PD = Parkinson disease, RBD = rapid eye movement sleep behavior disorder.

or dopamine transporter imaging using iodine 123-2 $\beta$ -carbomethoxy-3 $\beta$ -(4-iodophenyl)-*N*-(3-fluoropropyl)-nortropane ( $^{123}\text{I}$ -FP-CIT) SPECT were included. Patients were excluded if they (a) were taking medications that could influence polysomnography (eg, clonazepam, melatonin, or antidepressants); (b) were showing signs of cognitive impairment or diagnosed with other neurodegenerative disorders by means of neurologic examinations (ie, Unified Parkinson's Disease Rating Scale Part III, Mini-Mental State Examination, and Montreal Cognitive Assessment); (c) possessed at least a score of 1 on two or more of the 10 items in the Unified Parkinson's Disease Rating Scale Part III, at least a score of 2 on one item, or at least a score of 1 on resting tremor; and (d) did not agree to undergo neuroimaging study or failed to complete brain MRI due to motion. Patients who showed hydrocephalus or vascular ischemia in the white matter at brain MRI were also excluded. All participants were enrolled at the time of the MRI acquisition without knowledge of their phenconversion status.

During the study period, age- and sex-matched control participants were included based on the following criteria: (a) those who underwent clinical work-up including neurologic examination and brain MRI but who were not diagnosed with parkinsonism or RBD; (b) those who did not have any history of other neurologic disorders; and (c) those who were not taking any medication affecting the central nervous system. Those who showed hydrocephalus or vascular ischemic lesions in the white matter at MRI were also excluded.

Last, age- and sex-matched patients who were clinically diagnosed with de novo idiopathic PD according to the UK Parkinson's Disease Society Brain Bank criteria (28) and underwent neuroimaging study were enrolled in the group with PD. Among patients with PD, those who did not agree to undergo brain MRI and those who had hydrocephalus or vascular ischemia in the white matter at MRI were excluded.

Following the initial neurologic examination (Appendix S1), participants with RBD were followed up every 3–6 months and monitored for the development of any signs of neurodegenerative disorders, including sleep, motor, and cognitive status. Phenconversion was defined as the disease conversion from RBD to PD, dementia with Lewy bodies, or multiple system atrophy (7). Control participants were followed up yearly, and participants with PD were followed up every 3–6 months.

### Imaging Protocols and Assessment of Nigrostriatal Dopaminergic Degeneration

MRI protocols are described in Appendix S1. The scanning time for DTI was approximately 5 minutes 50 seconds. Using susceptibility-weighted imaging, we generated susceptibility map-weighted images to improve the detection of nigral hyperintensity (29). Normal nigral hyperintensity is seen as a focal hyperintense oval or linear hyperintense area in the dorsolateral aspect of the substantia nigra surrounded by hypointensity of the

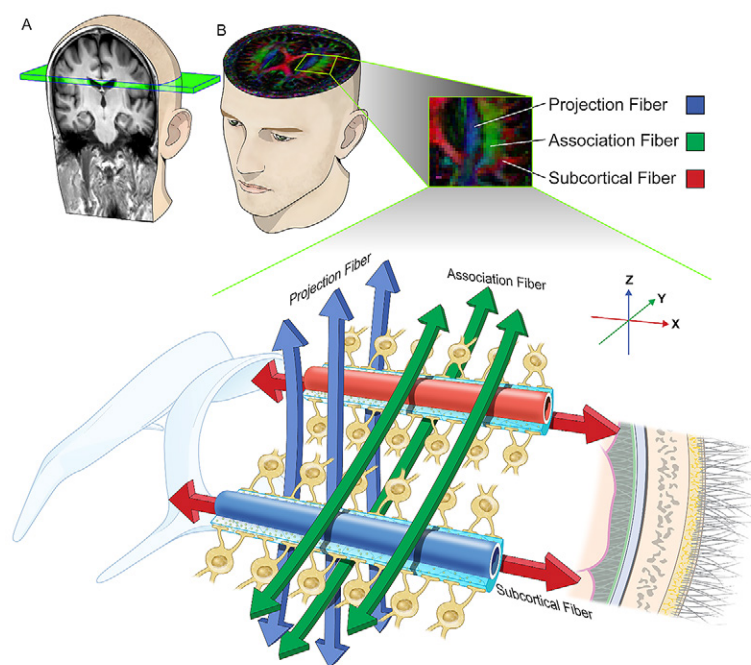


**Figure 2:** Schematic drawing of the principle underlying the diffusion-tensor imaging analysis along the perivascular space, or DTI-ALPS, method. (A) At the lateral ventricular body level, the neural fibers are identified on a (B) color-coded fractional anisotropy map. Perivascular water flows perpendicular to projection and association neural fibers. Therefore, diffusivity along the x-axis at these areas mostly reflects perivascular glymphatic flows.

iron (29–32). The loss of nigral hyperintensity is a reliable sign for nigral dopaminergic cell loss in PD, and it can be either present or absent in RBD depending on the degree of dopaminergic neurodegeneration (30–32). Two neuroradiologists (Y.J.B. and B.S.C., with 11 and 21 years of experience, respectively) assessed nigral hyperintensity in consensus on each side of the substantia nigra in the control, RBD, and PD groups; any disagreement was resolved by discussion.

$^{123}\text{I}$ -FP-CIT SPECT protocols are also summarized in Appendix S1. A nuclear medicine physician (Y.S.S., with 16 years of experience) assessed  $^{123}\text{I}$ -FP-CIT SPECT images. By visual inspection of the striatal dopamine transporter uptake, the reader determined the presence or absence of nigrostriatal dopaminergic degeneration.

### DTI-ALPS Processing

The DTI-ALPS method can be used to quantify glymphatic activity along the perivascular space with use of multidirectional diffusivity maps acquired from DTI data (19–25). The concept and specific method for DTI-ALPS are elaborated in Appendix S1 and Figures 2 and S1. After measurement of the diffusivities, the ALPS index was calculated to mitigate the influence of the periventricular white matter integrity and standardize measurements across individuals (see equation in Appendix S1) (19–25). The ALPS index is known to be close to 1 if the influence of water diffusion along the perivascular space is minimal or severely impaired. A larger ALPS index represents larger perivascular water diffusivity, meaning better glymphatic function (19–25). All measurements and the calculation of the ALPS index were

**Table 1: Baseline Demographic and Clinical Features of the Study Sample**

Characteristic	Control Group (n = 20)	Group with RBD (n = 20)	Group with PD (n = 20)	P Value
Age at onset (y)*	NA	65 (45–78) [61–68]	71 (49–81) [67–76]	.01
Age at imaging (y)*	73 (56–82) [68–76]	73 (53–82) [66–76]	72 (50–82) [68–77]	.96
Sex†				>.99
F	8	8	8	
M	12	12	12	
Hoehn and Yahr stage†	NA	NA		NA
I			10	
II			9	
III			1	
UPDRS-III score	0 (0–1)	0 (0–1)	16 (10–22)	<.001
MMSE score	28 (26–30)	28 (27–29)	27 (24–30)	.36
MoCA score	25.5 (24–28)	26 (25–28)	25 (24–28)	.30

Note.—Unless otherwise specified, data are medians, with ranges in parentheses. MMSE = Mini-Mental State Examination, MoCA = Montreal Cognitive Assessment, NA = not applicable, PD = Parkinson disease, RBD = rapid eye movement sleep behavior disorder, UPDRS-III = Unified Parkinson's Disease Rating Scale III.

\* Data in brackets are IQRs.

† Data are numbers of participants.

performed by two neuroradiologists (Y.J.B. and B.S.C.) independently and averaged for further analysis.

### Statistical Analysis

Clinical data between the control, RBD, and PD groups were compared using nonparametric tests and the  $\chi^2$  test. Interobserver agreement on the DTI-ALPS measurements between the two readers was evaluated using the interclass correlation coefficient (33). Differences in the DTI-ALPS measurements between the three groups were compared using the Kruskal-Wallis test followed by a post hoc Dunnnett T3 test (34). Particularly in the group with RBD, DTI-ALPS measurements were compared according to nigral hyperintensity status at susceptibility map-weighted imaging (SMWI) and visual inspection of the striatal dopaminergic degeneration at  $^{123}\text{I}$ -FP-CIT SPECT with use of the Mann-Whitney  $U$  test. In addition, the results from SMWI and  $^{123}\text{I}$ -FP-CIT SPECT were compared using the  $\chi^2$  test, and the concordance rate was calculated. Next, DTI-ALPS values were compared according to the phenoconversion status during follow-up with use of the Mann-Whitney  $U$  test. The diagnostic accuracy of SMWI and  $^{123}\text{I}$ -FP-CIT SPECT for the phenoconversion was calculated, and the diagnostic performance of the DTI-ALPS value for phenoconversion was tested using receiver operating characteristic curve analysis. Last, the risk of phenoconversion (ie, the risk of developing PD, dementia with Lewy bodies, or multiple system atrophy from RBD) according to the DTI-ALPS measurements as well as SMWI and  $^{123}\text{I}$ -FP-CIT SPECT was assessed with use of univariable and multivariable Cox proportional hazards models (35). The ability of the variables to help identify individuals at risk for phenoconversion was evaluated with the Harrell C-statistic and Akaike information criterion (36).  $P < .05$  was considered to indicate a

statistically significant difference. Multiple comparisons were corrected with use of the Bonferroni method. Statistical analyses were performed using SPSS (version 25.0; IBM), MedCalc 17.9 (MedCalc), and SAS software (version 9.3; SAS Institute).

## Results

### Participant Characteristics

A total of 60 consecutive participants were included: 20 participants with RBD (12 men, eight women; median age, 73 years [IQR, 66–76 years]), 20 age- and sex-matched control participants, and 20 age- and sex-matched participants with PD (Table 1).

### Interobserver Agreement for DTI-ALPS

Interobserver agreement was excellent for the ALPS index (interclass correlation coefficient, 0.85 [95% CI: 0.75, 0.91]) (Table S1).

### DTI-ALPS Measurements according to Clinical Diagnosis

The averaged DTI-ALPS values according to the participant groups are summarized in Tables 2 and 3 and Figure 3. The median ALPS index was lower in both the group with RBD (1.53) and the group with PD (1.49) than in controls (1.72) ( $P = .001$  and  $P < .001$ , respectively). However, the ALPS index showed no evidence of a difference between the groups with RBD and PD ( $P = .68$ ). Meanwhile, diffusivity along the y-axis in the association neural fibers, which is not regarded to reflect glymphatic function based on DTI-ALPS (19–25), also showed difference between the groups ( $P = .001$ ).

### DTI-ALPS Measurements in the Group with RBD according to SMWI and $^{123}\text{I}$ -FP-CIT SPECT

Among the 20 participants with RBD, 11 showed intact bilateral nigral hyperintensity, eight showed bilateral loss of nigral hyperintensity, and one showed intact right-side nigral hyperintensity but loss of left-side nigral hyperintensity (Fig 4A, 4B). In the group with RBD, the ALPS index was lower in those with either unilateral or bilateral loss of nigral hyperintensity (median, 1.39 [IQR, 1.25–1.49]) than in those with intact bilateral nigral hyperintensity (1.56 [IQR, 1.53–1.64];  $P = .02$ ).

Of the 20 participants with RBD, 15 underwent  $^{123}\text{I}$ -FP-CIT SPECT. Among them, nine had abnormal  $^{123}\text{I}$ -FP-CIT SPECT results that suggested nigrostriatal dopaminergic degeneration (Fig 4C, 4D). The concordance rate between the loss of the nigral hyperintensity at SMWI and abnormal  $^{123}\text{I}$ -FP-CIT SPECT results was 93% (Table S2). However, unlike with nigral hyperintensity, there was no evidence of a difference in the ALPS index according to  $^{123}\text{I}$ -FP-CIT SPECT



**Table 2: Comparison of the Diffusivities and ALPS Indexes among the Study Groups**

Parameter	Control Group (n = 20)	Group with RBD (n = 20)	Group with PD (n = 20)	P Value
D <sub>xproj</sub>	0.64 (0.53–0.87)	0.61 (0.47–0.75)	0.6 (0.42–0.69)	.05
D <sub>xassoc</sub>	0.65 (0.4–1)	0.55 (0.43–0.91)	0.56 (0.41–0.73)	.02
D <sub>xsubc</sub>	1.13 (0.85–1.51)	0.99 (0.73–1.3)	1.02 (0.86–1.27)	.04
D <sub>yproj</sub>	0.42 (0.31–0.55)	0.42 (0.32–0.61)	0.43 (0.36–0.55)	.61
D <sub>yassoc</sub>	0.99 (0.74–1.31)	0.77 (0.64–1.09)	0.98 (0.83–1.14)	.001*
D <sub>ysubc</sub>	0.64 (0.38–1.7)	0.86 (0.57–1.12)	0.69 (0.53–1)	.02
D <sub>zproj</sub>	1.13 (0.88–1.54)	1.05 (0.66–1.47)	1.12 (0.94–1.43)	.22
D <sub>zassoc</sub>	0.33 (0.21–0.58)	0.35 (0.28–0.49)	0.36 (0.23–0.43)	.53
D <sub>zsubc</sub>	0.55 (0.3–0.94)	0.65 (0.46–0.98)	0.59 (0.44–0.89)	.33
ALPS index	1.72 (1.32–2.07)	1.53 (1.19–1.94)	1.49 (1.1–1.73)	<.001*

Note.—Unless otherwise specified, data are medians, with ranges in parentheses. Diffusivities are presented as apparent diffusion coefficients ( $\times 10^{-3}$  mm<sup>2</sup>/sec). P values are derived from the comparison between all three groups with use of the Kruskal-Wallis test. ALPS = analysis along the perivascular space, D<sub>xassoc</sub> = diffusivity along the x-axis in the association fiber area, D<sub>xproj</sub> = diffusivity along the x-axis in the projection fiber area, D<sub>xsubc</sub> = diffusivity along the x-axis in the subcortical fiber area, D<sub>yassoc</sub> = diffusivity along the y-axis in the association fiber area, D<sub>yproj</sub> = diffusivity along the y-axis in the projection fiber area, D<sub>ysubc</sub> = diffusivity along the y-axis in the subcortical fiber area, D<sub>zassoc</sub> = diffusivity along the z-axis in the association fiber area, D<sub>zproj</sub> = diffusivity along the z-axis in the projection fiber area, D<sub>zsubc</sub> = diffusivity along the z-axis in the subcortical fiber area, PD = Parkinson disease, RBD = rapid eye movement sleep behavior disorder. \* P < .005 indicates statistically significant difference according to the multiple comparisons correction.

**Table 3: Subgroup Comparison of the Diffusivities and ALPS Indexes among the Study Groups**

Parameter and Groups for Comparison	P Value
D <sub>yassoc</sub> (ADC in $\times 10^{-3}$ mm <sup>2</sup> /sec)	
Control group vs group with RBD	.003*
Group with RBD vs group with PD	<.001*
ALPS index	
Control group vs group with RBD	.001*
Control group vs group with PD	<.001*

Note.—P values are derived from subgroup comparison at post hoc analysis. ADC = apparent diffusion coefficient, ALPS = analysis along the perivascular space, D<sub>yassoc</sub> = diffusivity along the y-axis in the association fiber area, PD = Parkinson disease, RBD = rapid eye movement sleep behavior disorder.

\* P < .005 indicates statistically significant difference according to the multiple comparisons correction.

findings (1.51 [normal SPECT findings] vs 1.34 [abnormal SPECT findings]; P = .27).

### Clinical Follow-up

The final clinical visits occurred in January 2022. The median interval between the first and last clinical visits was 37 months (IQR, 27–52 months). The median interval between the first clinical visit and MRI scan acquisition was 5 months (IQR, 3.8–10.8 months). The median duration from symptom onset (based on the history taking) to the first clinical visit was 54 months (IQR, 36–123 months), and that to last clinical visit was 108 months (IQR, 60–159 months). During follow-up, seven participants exhibited  $\alpha$ -synucleinopathy; six participants (four women and two men; median age, 76 years [IQR, 73–80 years]) developed PD (median, 6 months after imaging), and a 77-year-old man developed dementia with Lewy bodies (2 years after imaging). None

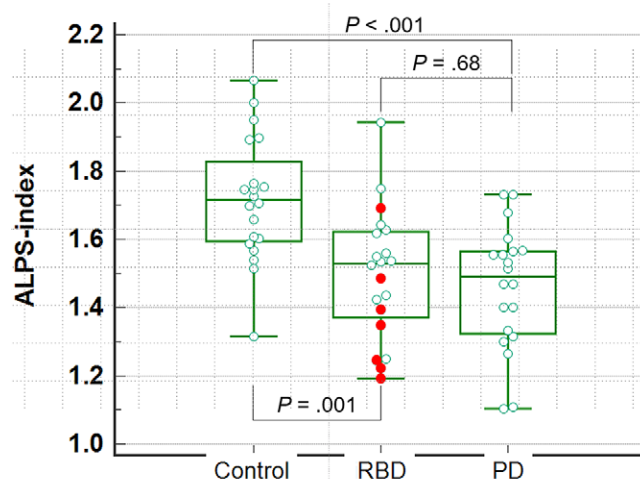


**Figure 3:** Box and whisker plot of the data from the diffusion-tensor imaging analysis along the perivascular space (ALPS) according to the clinical diagnosis. The values of ALPS index reflecting perivascular glymphatic flow in three groups (control group, participants with rapid eye movement sleep behavior disorder [RBD], and participants with Parkinson disease [PD]) are plotted (open circles). The data from participants with RBD showing phenoconversion to  $\alpha$ -synucleinopathy after the follow-up are marked (solid circles). The lower whisker, bottom of the box, horizontal line, top of the box, and upper whisker indicate the minimum value, first quartile, median, third quartile, and maximum value, respectively. P values for the comparisons between each group are shown in the figure.

of the control participants developed parkinsonism or dementia during the follow-up period. For participants with PD, the diagnosis remained unchanged during the follow-up.

Of seven participants with RBD who had phenoconversion, five showed loss of nigral hyperintensity at SMWI, and five had abnormal <sup>123</sup>I-FP-CIT SPECT results (Table S3). The sensitivity, specificity, and diagnostic accuracy for phenoconversion were 71% (five of seven participants; 95% CI: 29, 96), 69% (nine of 13 participants; 95% CI: 39, 91), and 70% (14

of 20 participants; 95% CI: 46, 88), respectively, at SMWI, and 71% (five of seven participants; 95% CI: 29, 96), 50% (four of eight participants; 95% CI: 16, 84), and 60% (nine of 15 participants; 95% CI: 32, 84), respectively, at  $^{123}\text{I}$ -FP-CIT SPECT.

Table 4 provides DTI-ALPS measurements according to phenoconversion status. The ALPS index provided a high area under the receiver operating characteristic curve in terms of diagnosing phenoconversion (Fig S2). However, after Bonferroni correction, there was no evidence of a difference between the ALPS index at the time of imaging in the group with RBD who exhibited phenoconversion and that in those who did not (1.35 vs 1.55;  $P = .02$ ). There also was no evidence of a difference in the ALPS index between the controls and the participants with RBD who did not show phenoconversion (1.72 vs 1.55;  $P = .02$ ) and between the participants with RBD who developed phenoconversion and the group with PD (1.35 vs 1.49,  $P = .20$ ).

The estimated phenoconversion-free probability in participants with RBD is shown in Figure 5. The risk of  $\alpha$ -synucleinopathy conversion in participants with RBD decreased with increasing ALPS index (hazard ratio, 0.57 per 0.1 increase in ALPS index [95% CI: 0.35, 0.93];  $P = .03$ ). The discriminability of the ALPS index was acceptable (C-index, 0.72; Akaike information criterion, 32.5).

On the other hand, the phenoconversion risk in participants with RBD showed no evidence of a difference according to SMWI (hazard ratio, 4.20 [95% CI: 0.80, 22.1];  $P = .09$ ) and  $^{123}\text{I}$ -FP-CIT SPECT (hazard ratio, 2.09 [95% CI: 0.40, 11.0];  $P = .39$ ). Additionally, the subsequent multivariable analysis using the ALPS index combined with SMWI showed no evidence of a difference when adding nigral hyperintensity to the risk prediction (hazard ratio, 0.63 [95% CI: 0.35, 1.13];  $P = .12$ ).

## Discussion

Glymphatic dysfunction may contribute to the development of  $\alpha$ -synucleinopathies in the brain. In this prospective study, we found reduced brain glymphatic activity at diffusion-tensor MRI in study participants with rapid eye movement sleep behavior disorder (RBD) before the onset of parkinsonism. The analysis along the perivascular space (ALPS) index reflecting perivascular glymphatic flow was decreased in the group with RBD compared with controls (1.53 vs 1.72;  $P = .001$ ). A decreased risk of phenoconversion was demonstrated with increasing ALPS

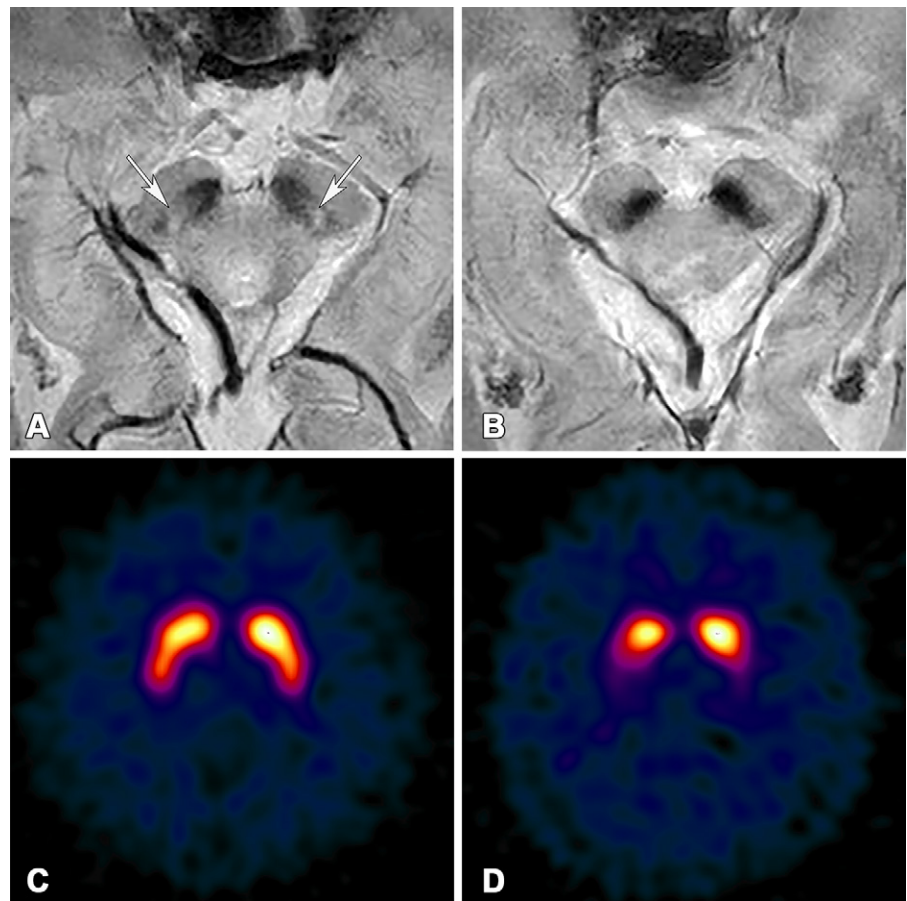


**Figure 4:** Representative images of normal and abnormal findings at susceptibility map-weighted imaging (SMWI) and iodine 123-2 $\beta$ -carbomethoxy-3 $\beta$ -(4-iodophenyl)-N-(3-fluoropropyl)-nortropane ( $^{123}\text{I}$ -FP-CIT) SPECT in participants with rapid eye movement sleep behavior disorder. **(A)** SMWI scan in a 69-year-old woman shows intact bilateral nigral hyperintensities (arrows) that are considered a normal finding. **(B)** SMWI scan in a 75-year-old woman shows abnormal loss of bilateral nigral hyperintensities. **(C)**  $^{123}\text{I}$ -FP-CIT SPECT image in the same participant as in **A** shows preserved bilateral striatal uptakes of  $^{123}\text{I}$ -FP-CIT, which are considered a normal result from visual inspection of nigrostriatal dopaminergic degeneration at SPECT. **(D)**  $^{123}\text{I}$ -FP-CIT SPECT image in the same participant as in **B** shows abnormally reduced bilateral striatal uptakes of  $^{123}\text{I}$ -FP-CIT, reflecting the process of nigrostriatal dopaminergic degeneration.

index (hazard ratio, 0.57 per 0.1 increase in ALPS index [95% CI: 0.35, 0.93];  $P = .03$ ). Therefore, glymphatic impairment is presumed to start at the preclinical stage, and glymphatic dysfunction may contribute to the phenoconversion from RBD to  $\alpha$ -synucleinopathy. Preserved glymphatic activity with higher ALPS index may also act as a neuroprotective mechanism against the development of  $\alpha$ -synucleinopathy.

The DTI-ALPS method provides noninvasive quantification of glymphatic function (19–24). It has its own complementary measures to compensate for the effect from major neural tracts and minor neural bundles in the white matter and from individual differences in white matter diffusivity (19–24). The validation of DTI-ALPS has been provided in a previous human-based study that performed both DTI-ALPS and intrathecal contrast agent injection for the glymphatic analysis (25). In that study, the ALPS index was correlated with delayed glymphatic clearance using percentage changes of the signal unit ratio in the brain (25). Another study has found the trend of the age-dependent change in the ALPS index to be consistent with previous

**Table 4: Comparison of the Diffusivities and ALPS Indexes in the Group with RBD according to Conversion**

Parameter	Conversion Group (n = 7)	Nonconversion Group (n = 13)	P Value
D <sub>xproj</sub>	0.56 (0.47–0.75)	0.61 (0.54–0.68)	.49
D <sub>xassoc</sub>	0.5 (0.43–0.91)	0.58 (0.46–0.78)	.31
D <sub>xsubc</sub>	0.99 (0.73–1.3)	1.03 (0.87–1.22)	.88
D <sub>yproj</sub>	0.49 (0.39–0.61)	0.42 (0.32–0.47)	.05
D <sub>yassoc</sub>	0.76 (0.67–0.89)	0.9 (0.65–1.09)	.35
D <sub>ysubc</sub>	0.91 (0.57–1.12)	0.74 (0.57–0.98)	.21
D <sub>zproj</sub>	1.01 (0.82–1.28)	1.07 (0.66–1.47)	.49
D <sub>zassoc</sub>	0.35 (0.28–0.49)	0.35 (0.29–0.46)	>.99
D <sub>zsubc</sub>	0.66 (0.54–0.88)	0.64 (0.46–0.98)	.44
ALPS index	1.35 (1.19–1.69)	1.55 (1.25–1.94)	.02

Note.—Unless otherwise specified, data are medians, with ranges in parentheses. Diffusivities are presented as apparent diffusion coefficients ( $\times 10^{-3}$  mm<sup>2</sup>/sec). *P* values were derived with use of the Mann-Whitney *U* test. *P* < .005 indicates statistically significant difference according to the multiple comparisons correction. ALPS = analysis along the perivascular space,

D<sub>xassoc</sub> = diffusivity along the x-axis in the association fiber area, D<sub>xproj</sub> = diffusivity along the x-axis in the projection fiber area, D<sub>xsubc</sub> = diffusivity along the x-axis in the subcortical fiber area, D<sub>yassoc</sub> = diffusivity along the y-axis in the association fiber area, D<sub>yproj</sub> = diffusivity along the y-axis in the projection fiber area, D<sub>ysubc</sub> = diffusivity along the y-axis in the subcortical fiber area, D<sub>zassoc</sub> = diffusivity along the z-axis in the association fiber area, D<sub>zproj</sub> = diffusivity along the z-axis in the projection fiber area, D<sub>zsubc</sub> = diffusivity along the z-axis in the subcortical fiber area, RBD = rapid eye movement sleep behavior disorder.

observations in preclinical and human-based studies using an intrathecal tracer, providing further verification of the DTI-ALPS (37–39). Additionally, the high intra- and interobserver agreement and the robust reproducibility of DTI-ALPS measurements for the fixed imaging parameters have been proven in several published studies (21,25,40). Moreover, DTI can be performed within several minutes, enabling the monitoring of glymphatic activity over time. Accordingly, DTI-ALPS has been applied to a series of neurodegenerative disorders, including PD, Alzheimer disease, and normal pressure hydrocephalus, and has demonstrated a correlation with clinical scores (19–24). Therefore, the DTI-ALPS method is suitable for patients with RBD who are in the prodromal stage and require repeated follow-ups to monitor disease progression longitudinally.

It has been shown that greater glymphatic clearance occurs during sleep compared with wakefulness. Therefore, dynamic relationships between sleep, glymphatic function, and the development of neurodegenerative disorders have been postulated (26,41–43). Glymphatic dysfunction among patients with RBD may contribute to the development of PD by reducing excretion of  $\alpha$ -synuclein from brain parenchyma into extracellular spaces (1–4,44,45). Recently, Si et al (10) suggested the possibility of brain waste drainage dysfunction in RBD by assessing MRI-visible perivascular space burden, and another two studies have reported reduced ALPS index in patients with RBD compared with healthy controls (11,12). However, to

our knowledge, none have followed up the patients with RBD and evaluated the connection between glymphatic dysfunction and phenoconversion risk.

In our study, we identified the reduced glymphatic activity according to lower ALPS index in the RBD group than in controls. Other than ALPS index, diffusivity along the y-axis in the association neural fibers also showed difference between the RBD and control groups. This diffusivity is not the diffusivity parallel to the perivascular water flow; therefore, it is fair to believe that this difference was not from the glymphatic function, but from other factors that can contribute to the diffusion along the y-axis. Indeed, several previous studies have explained the differences in the diffusion values along the y-axis by the influence from white matter degeneration or individual variation in white matter integrity (19–21).

To date, a few imaging techniques have been applied to evaluate the prodromal stage of  $\alpha$ -synucleinopathy, and susceptibility-weighted imaging and dopamine transporter imaging have been widely used to demonstrate the process of nigrostriatal dopaminergic degeneration. A previous study showed that participants with RBD with loss of nigral hyperintensity may have worsened nigrostriatal dopaminergic degeneration at dopamine transporter imaging (31). Importantly, in that study, participants with RBD with loss of nigral hyperintensity showed higher conversion risks than those without (31). Therefore, loss of nigral hyperintensity may act as a predictor for phenoconversion (31). Correspondently, the ALPS index in our study was lower in participants with RBD with loss of nigral hyperintensity than in those without, and participants with RBD with lower ALPS index were at high risk of phenoconversion. This suggests an association between nigral hyperintensity status and glymphatic function. Glymphatic impairment may be worse in patients with progressed nigrostriatal dopaminergic degeneration and thus a higher risk of future phenoconversion. Nonetheless, the ALPS index showed no evidence of a difference according to <sup>123</sup>I-FP-CIT SPECT, possibly due to the small sample size.

The DTI-ALPS method is expected to serve as an imaging biomarker for RBD. By its use in assessing glymphatic function, DTI-ALPS may assist in selecting proper candidates for neuroprotective therapy using monoclonal antibodies for  $\alpha$ -synuclein (46). To enhance the effect of immunization to prevent the development of  $\alpha$ -synucleinopathy from RBD, intact glymphatic drainage to eliminate  $\alpha$ -synuclein from the brain is a prerequisite, and DTI-ALPS can be used to predict and monitor the neuroprotective effect. Taking these together, we suggest that DTI-ALPS can serve as an MRI biomarker for RBD and a predictor for  $\alpha$ -synucleinopathy development.

Our study had several limitations. First, there was a small number of participants with RBD diagnosed with use of polysomnography, even at a nationwide tertiary hospital. The number of phenoconversion events was also small. Because RBD has a prevalence of approximately 1% in the population aged older than 60 years and there is a latency of 10 years or more from symptom onset to phenoconversion (9), the small number of participants in the RBD cohort is a fundamental limitation. Second, only 15 of the 20 participants with RBD underwent <sup>123</sup>I-FP-CIT SPECT. Third, the total follow-up period (median, 37



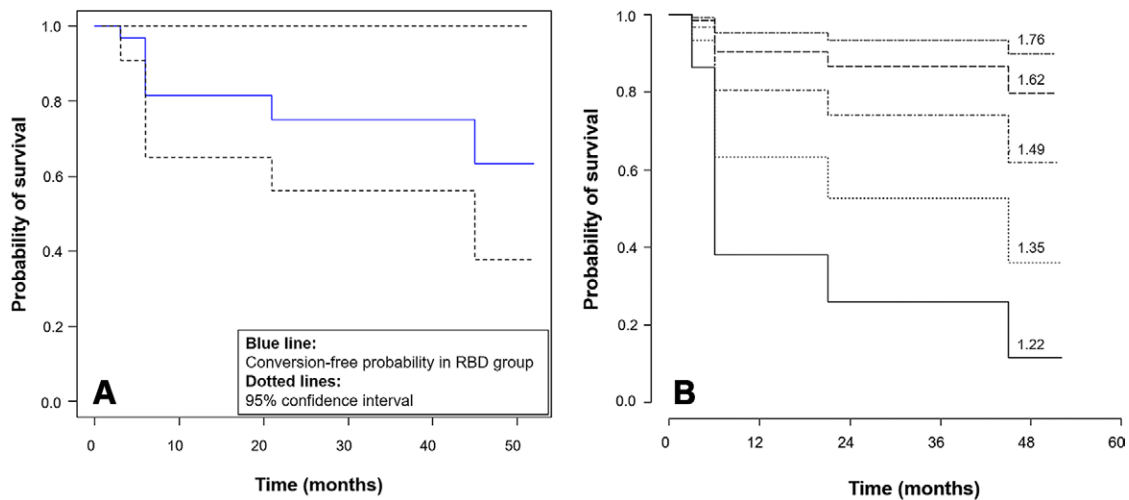


**Figure 5:** Cox regression analysis of the risk of  $\alpha$ -synucleinopathy conversion in participants with isolated rapid eye movement sleep behavior disorder (RBD). **(A)** The survival probability graph from Cox regression analysis of a total of 20 participants in the group with RBD shows the conversion-free probability with the median analysis along the perivascular space (ALPS) index. **(B)** Survival graph shows the conversion-free probability according to the specific ALPS index. The conversion-free probability is higher with higher ALPS index (values shown on the graph).

months [IQR, 27–52 months]) was short for establishing the role of glymphatic function in disease progression. Fourth, we conducted only a visual qualitative analysis at SPECT, since a larger sample size is necessary for a regression analysis of the quantitative  $^{123}\text{I}$ -FP-CIT uptakes. Last, although DTI-ALPS can be used to isolate perivascular glymphatic diffusivity, the measurement is based on the free diffusion parallel to the x-axis, and it cannot reflect the glymphatic flow along the y-axis or z-axis (19–25). The glymphatic function in the periventricular area may not reflect glymphatic alterations directly affecting the nigrostriatal pathway. Therefore, future studies with a larger number of participants with RBD who have been assessed with DTI, susceptibility-weighted imaging, and quantitative SPECT analysis and followed up for longer periods are needed. In addition, advanced MRI techniques may enable noninvasive glymphatic measurements in variable anatomic structures in the future.

In conclusion, assessing brain glymphatic dysfunction in individuals with isolated rapid eye movement sleep behavior disorder (RBD) with use of diffusion-tensor imaging (DTI) analysis along the perivascular space (ALPS) revealed glymphatic alterations. The reduction of glymphatic activity was more severe in individuals with phenoconversion to  $\alpha$ -synucleinopathies. Therefore, DTI-ALPS may assist in identifying individuals with RBD at a high risk of phenoconversion before the onset of parkinsonian symptoms.

**Acknowledgments:** We thank InSeong Kim, MS (Siemens Healthineers), for the DTI-ALPS analyzer. We thank the Medical Research Collaborating Center at Seoul National University Bundang Hospital for consultation with the statistical analyses. We thank Editage ([www.editage.co.kr](http://www.editage.co.kr)) for English language editing. We acknowledge and thank Dong Su Jang, PhD, and studioMID (Medical Illustration & Design) for creating the illustrations.

**Author contributions:** Guarantors of integrity of entire study, Y.J.B., J.M.K., N.R.; study concepts/study design or data acquisition or data analysis/interpretation, all authors; manuscript drafting or manuscript revision for important intellectual content, all authors; approval of final version of submitted manuscript, all authors; agrees to ensure any questions related to the work are appropriately resolved, all authors;

literature research, Y.J.B., J.M.K., B.S.C., N.R., Y.S.S., I.Y.Y., J.H.K.; clinical studies, Y.J.B., J.M.K.; experimental studies, J.M.K., B.S.C., N.R., Y.S.S., Y.N., I.Y.Y., J.H.K.; statistical analysis, Y.J.B., J.M.K.; and manuscript editing, all authors

**Data sharing:** Data generated or analyzed during the study are available from the corresponding author by request.

**Disclosures of conflicts of interest:** Y.J.B. No relevant relationships. J.M.K. No relevant relationships. B.S.C. No relevant relationships. N.R. No relevant relationships. Y.S.S. No relevant relationships. Y.N. No relevant relationships. I.Y.Y. No relevant relationships. S.J.C. No relevant relationships. J.H.K. No relevant relationships.

## References

- Jessen NA, Munk AS, Lundgaard I, Nedergaard M. The glymphatic system: a beginner's guide. *Neurochem Res* 2015;40(12):2583–2599.
- Rasmussen MK, Mestre H, Nedergaard M. The glymphatic pathway in neurological disorders. *Lancet Neurol* 2018;17(11):1016–1024.
- Lliff JJ, Wang M, Liao Y, et al. A paravascular pathway facilitates CSF flow through the brain parenchyma and the clearance of interstitial solutes, including amyloid  $\beta$ . *Sci Transl Med* 2012;4(147):147ra111.
- Sundaram S, Hughes RL, Peterson E, et al. Establishing a framework for neuropathological correlates and glymphatic system functioning in Parkinson's disease. *Neurosci Biobehav Rev* 2019;103:305–315.
- Iranzo A, Tolosa E, Gelpi E, et al. Neurodegenerative disease status and post-mortem pathology in idiopathic rapid-eye-movement sleep behaviour disorder: an observational cohort study. *Lancet Neurol* 2013;12(5):443–453.
- Postuma RB. Prodromal Parkinson's disease—using REM sleep behavior disorder as a window. *Parkinsonism Relat Disord* 2014;20(Suppl 1):S1–S4.
- Zhang H, Iranzo A, Högl B, et al. Risk factors for phenoconversion in rapid eye movement sleep behavior disorder. *Ann Neurol* 2022;91(3):404–416.
- Postuma RB, Adler CH, Dugger BN, et al. REM sleep behavior disorder and neuropathology in Parkinson's disease. *Mov Disord* 2015;30(10):1413–1417.
- Postuma RB, Iranzo A, Hu M, et al. Risk and predictors of dementia and parkinsonism in idiopathic REM sleep behaviour disorder: a multicentre study. *Brain* 2019;142(3):744–759.
- Si XL, Gu LY, Song Z, et al. Different perivascular space burdens in idiopathic rapid eye movement sleep behavior disorder and Parkinson's disease. *Front Aging Neurosci* 2020;12:580853.
- Lee DA, Lee HJ, Park KM. Glymphatic dysfunction in isolated REM sleep behavior disorder. *Acta Neurol Scand* 2022;145(4):464–470.
- Si X, Guo T, Wang Z, et al. Neuroimaging evidence of glymphatic system dysfunction in possible REM sleep behavior disorder and Parkinson's disease. *NPJ Parkinsons Dis* 2022;8(1):54.



13. Lee MK, Cho SJ, Bae YJ, Kim JM. MRI-based demonstration of the normal glymphatic system in a human population: a systematic review. *Front Neurol* 2022;13:827398.
14. Eide PK, Ringstad G. MRI with intrathecal MRI gadolinium contrast medium administration: a possible method to assess glymphatic function in human brain. *Acta Radiol Open* 2015;4(11):2058460115609635.
15. de Leon MJ, Li Y, Okamura N, et al. Cerebrospinal fluid clearance in Alzheimer disease measured with dynamic PET. *J Nucl Med* 2017;58(9):1471–1476.
16. Ringstad G, Varnehol SAS, Eide PK. Glymphatic MRI in idiopathic normal pressure hydrocephalus. *Brain* 2017;140(10):2691–2705.
17. Nguyen NC, Molnar TT, Cummin LG, Kanal E. Dentate nucleus signal intensity increases following repeated gadobenate dimeglumine administrations: a retrospective analysis. *Radiology* 2020;296(1):122–130.
18. McDonald RJ, Kallmes DF. Signal intensity changes at MRI following GBCA exposure: incidental finding or cause for concern? *Radiology* 2020;296(1):131–133.
19. Taoka T, Masutani Y, Kawai H, et al. Evaluation of glymphatic system activity with the diffusion MR technique: diffusion tensor image analysis along the perivascular space (DTI-ALPS) in Alzheimer's disease cases. *Jpn J Radiol* 2017;35(4):172–178.
20. Yokota H, Vijayasarathi A, Cecik M, et al. Diagnostic performance of glymphatic system evaluation using diffusion tensor imaging in idiopathic normal pressure hydrocephalus and mimickers. *Curr Gerontol Geriatr Res* 2019;5675014.
21. Bae YJ, Choi BS, Kim JM, Choi JH, Cho SJ, Kim JH. Altered glymphatic system in idiopathic normal pressure hydrocephalus. *Parkinsonism Relat Disord* 2021;82:56–60.
22. Chen HL, Chen PC, Lu CH, et al. Associations among cognitive functions, plasma DNA, and diffusion tensor image along the perivascular space (DTI-ALPS) in patients with Parkinson's disease. *Oxid Med Cell Longev* 2021;2021:4034509.
23. Ma X, Li S, Li C, et al. Diffusion tensor imaging along the perivascular space index in different stages of Parkinson's disease. *Front Aging Neurosci* 2021;13:773951.
24. Barisano G, Lynch KM, Sibilia F, et al. Imaging perivascular space structure and function using brain MRI. *Neuroimage* 2022;257:119329.
25. Zhang W, Zhou Y, Wang J, et al. Glymphatic clearance function in patients with cerebral small vessel disease. *Neuroimage* 2021;238:118257.
26. Siow TY, Toh CH, Hsu JL, et al. Association of sleep, neuropsychological performance, and gray matter volume with glymphatic function in community-dwelling older adults. *Neurology* 2022;98(8):e829–e838.
27. American Academy of Sleep Medicine. *International Classification of Sleep Disorders*. 3rd ed. American Academy of Sleep Medicine, 2014.
28. Hughes AJ, Daniel SE, Kilford L, Lees AJ. Accuracy of clinical diagnosis of idiopathic Parkinson's disease: a clinico-pathological study of 100 cases. *J Neurol Neurosurg Psychiatry* 1992;55(3):181–184.
29. Nam Y, Gho SM, Kim DH, Kim EY, Lee J. Imaging of nigrosome 1 in substantia nigra at 3T using multiecho susceptibility map-weighted imaging (SMWI). *J Magn Reson Imaging* 2017;46(2):528–536.
30. De Marzi R, Seppi K, Högl B, et al. Loss of dorsolateral nigral hyperintensity on 3.0 tesla susceptibility-weighted imaging in idiopathic rapid eye movement sleep behavior disorder. *Ann Neurol* 2016;79(6):1026–1030.
31. Bae YJ, Kim JM, Kim KJ, et al. Loss of substantia nigra hyperintensity at 3.0-T MR imaging in idiopathic REM sleep behavior disorder: comparison with <sup>123</sup>I-FP-CIT SPECT. *Radiology* 2018;287(1):285–293.
32. Brammerloh M, Kirilina E, Alkemade A, et al. Swallow tail sign: revisited. *Radiology* 2022;305(3):674–677.
33. McGraw KO, Wong SP. Forming inferences about some intraclass correlation coefficients. *Psychol Methods* 1996;1(1):30–46.
34. Lee S, Lee DK. What is the proper way to apply the multiple comparison test? *Korean J Anesthesiol* 2018;71(5):353–360. [Published correction appears in *Korean J Anesthesiol* 2020;73(6):572.]
35. Heinze G, Schemper M. A solution to the problem of monotone likelihood in Cox regression. *Biometrics* 2001;57(1):114–119.
36. Harrell FE Jr, Lee KL, Mark DB. Multivariable prognostic models: issues in developing models, evaluating assumptions and adequacy, and measuring and reducing errors. *Stat Med* 1996;15(4):361–387.
37. Taoka T, Ito R, Nakamichi R, et al. Diffusion-weighted image analysis along the perivascular space (DWI-ALPS) for evaluating interstitial fluid status: age dependence in normal subjects. *Jpn J Radiol* 2022;40(9):894–902.
38. Kress BT, Iliff JJ, Xia M, et al. Impairment of paravascular clearance pathways in the aging brain. *Ann Neurol* 2014;76(6):845–861.
39. Zhou Y, Cai J, Zhang W, et al. Impairment of the glymphatic pathway and putative meningeal lymphatic vessels in the aging human. *Ann Neurol* 2020;87(3):357–369.
40. Taoka T, Ito R, Nakamichi R, et al. Reproducibility of diffusion tensor image analysis along the perivascular space (DTI-ALPS) for evaluating interstitial fluid diffusivity and glymphatic function: CHanges in Alps index on Multiple conditiON acquisition eXperiment (CHAMONIX) study. *Jpn J Radiol* 2022;40(2):147–158.
41. Lee S, Yoo RE, Choi SH, et al. Contrast-enhanced MRI T1 mapping for quantitative evaluation of putative dynamic glymphatic activity in the human brain in sleep-wake states. *Radiology* 2021;300(3):661–668.
42. Eide PK, Pripp AH, Berge B, Hrubos-Strøm H, Ringstad G, Valnes LM. Altered glymphatic enhancement of cerebrospinal fluid tracer in individuals with chronic poor sleep quality. *J Cereb Blood Flow Metab* 2022;42(9):1676–1692.
43. Kylkilahti TM, Berends E, Ramos M, et al. Achieving brain clearance and preventing neurodegenerative diseases—a glymphatic perspective. *J Cereb Blood Flow Metab* 2021;41(9):2137–2149.
44. Iliff JJ, Chen MJ, Plog BA, et al. Impairment of glymphatic pathway function promotes tau pathology after traumatic brain injury. *J Neurosci* 2014;34(49):16180–16193.
45. Peng W, Achariy TM, Li B, et al. Suppression of glymphatic fluid transport in a mouse model of Alzheimer's disease. *Neurobiol Dis* 2016;93:215–225.
46. Videnovic A, Ju YS, Arnulf I, et al. Clinical trials in REM sleep behavioural disorder: challenges and opportunities. *J Neurol Neurosurg Psychiatry* 2020;91(7):740–749.